Beni-Suef University Journal of Basic and Applied Sciences

RESEARCH

Open Access

Combination of decaffeinated green coffee and decaffeinated green tea ameliorates cardiomyopathy through cardiotrophin-1-dependent expression regulation in a metabolic syndrome rat model: a proposed mechanism

Mohammad Saifur Rohman[1,2], Mifetika Lukitasari[2,3,7*], Mukhamad Nur Kholis[2,4], Nila Aisyah Wahyuni[2,4], Beryl Reinaldo Chandra[2,4], Feri Eko Hermanto[5,6] and Nashi Widodo[2,8]

Abstract

Background Cardiovascular diseases (CVD) are the primary medical manifestation of metabolic syndrome (MetS). Hypoxia is also involved in the pathogenesis of CVD. Since dietary intervention significantly improved the physiological condition in MetS, the development of functional food to complement conventional medical therapy is essential. Among several standard consumable products, decaffeinated green tea (DGT) and decaffeinated green coffee (DGC) have excellent activity in managing MetS-induced CVD. However, the mechanism underlying their protective activity is poorly understood. This study aimed to understand the cardio-protective activity of DGT, DGC, and a combination of the two (DGT + DGC) in managing MetS-induced CVD in vivo and in silico.

Results The MetS condition led to the upregulation of *Cardiotrophin-1* (*CT-1*), *Signal Transducer and Activator of Transcription 3* (*STAT3*), *GATA binding protein 4* (*GATA4*), and *B-type Natriuretic Peptide* (*BNP*) beyond the levels of the normal (N) group, while administration of DGT, DGC, and DGT + DGC significantly decreased the expression of those genes compared with the levels of the N group ($p < 0.05$). The computational analysis showed that the protective role of DGT, DGC, and DGT + DGC might be achieved through AKT1 inhibition by several bioactive components present in DGT and DGC. The analysis also defined the improvement in cardio-protective activity by combining DGT and DGC.

Conclusions The administration of DGT, DGC, or DGT + DGC repaired cardiac dysfunction parameters through indirect regulation of the CT-1 signaling axis by inhibiting AKT1 activity.

Keywords AKT1, Cardiotrophin-1, Cardiovascular diseases, Decaffeinated green coffee, Decaffeinated green tea, Metabolic syndrome

*Correspondence:
Mifetika Lukitasari
mifetika.fk@ub.ac.id
Full list of author information is available at the end of the article

1 Background

Changes in lifestyle, nutrition, and social environments in modern society positively correlate with the global escalation of the prevalence obesity, insulin resistance (IR), diabetes, dyslipidemia, and hypertension [1]. The occurrence of those abnormalities is generally known as metabolic syndrome (MetS) [1]. Additionally, development of cardiovascular disease (CVD) in individuals with MetS indicates a poor prognoses compared to the individual without it [2]. The combination among several aforementioned features of MetS increases the risk and severity of a broad spectrum of CVD [3].

Dysregulation of metabolic activity associated with glucose and lipid metabolism is the primary causative agent in the development of MetS. A recent study revealed the overexpression of cardiotrophin-1 (CT-1) to be linked to MetS-induced CVD [4, 5]. CT-1 belongs to the interleukin-6 (IL-6) cytokine family that has a crucial role in glucose and lipid metabolism, obesity, IR pathogenesis, and, importantly, cardiomyopathy pathogenesis [4, 6, 7]. CT-1 induces signal transduction via the membrane glycoprotein 130 (gp130) receptor system [8]. Activation of gp130 induces the expression of the signal transducer and activator of transcription 3 (STAT3) [9]. Then, STAT3 expression upregulates the transcription factor GATA4 [10] and leads to the transcription of the B-type natriuretic peptide (*BNP*) gene [11]. Interestingly, the dysregulated level of BNP in the serum was an independent predictor for CVD mortality and might serve as a target for medium to long-term preventive therapies [12]. Thus, the inter-dependent pathway of those genes provides an opportunity to regulate MetS-induced CVD pathophysiology.

Lifestyle modification, particularly dietary intervention, plays a significant role in physiological improvement under MetS conditions beyond conventional medical therapy [13]. Among several available natural products, Decaffeinated Green Tea (DGT) and Decaffeinated Green Coffee (DGC) have the potential bioactivity in maintaining physiological homeostasis. DGT and DGC have been shown to individually improve the physiological balance in MetS conditions and display cardio-protective effects [14–16]. In addition, a combination of DGT + DGC was also reported to have physiological benefits by ameliorating MetS through regulating lipid and glucose metabolism, IR, and inflammation [17–20]. Although the cardio-protective effect of the DGT + DGC administration has been elucidated [19, 21], the biomechanism underlying it remains unknown. Therefore, this study will explore the protective effect of DGT, DGC, and DGT + DGC against cardiomyopathy in vivo and in silico.

2 Methods

2.1 Extraction of DGC and DGT

The DGC and DGT were extracted according to the protocol described by Rohman et al. [17]. The coffee bean was obtained from the Dampit coffee plantation in Malang, Indonesia (800 MAMSL). *Coffea canephora* var. *robusta* was light roasted on an automatic coffee roaster (N500i) at 180–200 °C until the first crack. Afterwards, the coffee bean was grinded using a coffee grinder and macerated with ethanol 95% to produce the crude extract. A filter cloth was used to separate the liquid phase from the solid phase of the crude extract. Finally, remaining solvent in the liquid phase was rotary evaporated at 40 °C (RV10 autoV, IKA). Column chromatography was performed using silica gel C18 17% (SiliaBond® C18, SiliCycle Inc) as a static phase to obtain the DGC. Then, the filtered product was evaporated.

The green tea was obtained from Sukawana green tea plantation, Bandung, Indonesia (1550 MAMSL). A total of 500 g of green tea leaf were dried in a cabinet dryer at 50 °C for eight hours to produce green tea with an 8–10% water content, which was then quantified using gravimetric analysis. The dried green tea leaves then grinded and boiled for 30 min at 80 °C. A filter cloth was applied to separate the liquid and solid phase of macerated green tea leaves. The liquid phase was then concentrated using a rotary evaporator at 40 °C. The column chromatography was used to obtain the bioactive compounds (SiliaBond® C18, SiliCycle Inc.), and the obtained yield was then evaporated to obtain the DGT.

2.2 Animal model

The animal model for MetS was developed according to a previously described method [18, 22]. Twenty-five male Sprague–Dawley rats aged 2–3 months old with an average weight of 250–300 g were randomly assigned into the following five groups: Normal (N), MetS, DGC administration, DGT administration, and DGT + DGC administration ($n = 5$ per group). MetS rats were fed a high-fat and high-sucrose (HFHS) diet for eight weeks with the injection of STZ (30 mg/Kg BW) intraperitoneally in the second week during the HFHS feeding, while the N rats were fed a regular diet. The DGC group was orally administered a single GC extract at a dose of 200 mg/Kg BW, the DGT group with a single DGT extract at a dose of 300 mg/Kg BW, and the DGC + DGT group with DGC + DGT extract at a dose of 200 and 300 mg/Kg BW, respectively. All treatments were given orally using a feeding tube every afternoon (03.00–05.00 PM) for nine

weeks. At the end of the treatment, the rats were euthanized with diethyl ether, and the hearts were harvested and preserved in an RNA buffer solution to keep RNA integrity.

2.3 RNA isolation, cDNA transcription, and cDNA amplification

According to the manufacturer's instructions, RNA was isolated from cardiac tissue using the TRIzol® reagent (Intron Biotechnology, South Korea). RNA was reverse transcribed into cDNA using a ReverTra Ace-α Kit (Ref FSK-101, Toyobo, Japan). The relative expression of *CT-1*, *STAT3*, *BNP*, and *GATA4* was analyzed through touchdown PCR amplification using a LightCycler 96 system (Takara, Japan). β-actin (*Actb*) was selected as the standard expression measurement for each gene. The primer sequences for each analyzed gene are described in Table 1. The amplification program was set as follows: 94 °C for 10 s, 57 °C for 30 s, 55 °C for 60 s, and 52 °C for 10 min. The PCR program was run for 36 cycles. Agarose gel electrophoresis was performed to analyze the amplified cDNA. The density of the visualized bands was then quantified using ImageJ software to determine the relative expression of the target genes.

2.4 Data analysis

The expression of each target gene was calculated relative to β-actin's expression. The data were then statistically analyzed using one-way ANOVA and Duncan's post hoc test. The data were determined as significantly different if $p < 0.05$.

2.5 Compound and protein structure retrieval

The compounds' three-dimensional (3D) structures were downloaded from the PubChem database. Cafestol, chlorogenic acid, citric acid, kahweol, quinic acid, and trigonelline were selected as the bioactive compounds from DGC [23], and epicatechin (EC), epicatechin gallate (ECG), epigallocatechin (EGC), and epigallocatechin gallate (EGCG) were determined as the main bioactive compounds of DGT [24]. Meanwhile, the 3D structure of proteins was retrieved from the RCSB protein data bank (PDB) with the following PDB identity (ID): AKT1 (3O96) and HIF-1α (4H6J). Before the docking process, the protein structures were prepared by deleting the water molecules, unwanted protein chains, and pre-attached ligands.

Table 1 The primer sequence for each target gene in this study

Gene	Primer sequence (5′ to 3′)	
	Forward	Reverse
CT-1	GGTGTGTTGAAGGAAACAGG	GTTGCTGCACATATTCCTCC
STAT3	GCAGCAACTCAGATCACTGAA	GCACCGAAAAGGCTGTTAC
BNP	CTGCTGGAGCTGATAAGAGAA	CGGTCTATCTTCTGCCCAAA
GATA4	CCCCAATCTCGATATGTTTGATG	TGGTTTGAATCCCCTCCTTC
β-actin	TGAGAGGGAAATCGTGCGTGA CAT	ACCGCTCATTGCCGATAG TGATGA

2.6 Molecular docking

AutoDock Vina [25] was employed for the docking process in the PyRx 0.8 user interface [26]. The compounds' structures were inserted, their energy minimized, and converted to AutoDock Vina's ligand through the Open-Babel plugin [27]. The proteins, as well as the macromolecules, were set as rigid entities, while the ligands were set as flexible molecules. As per previous studies, the docking was specified at the inhibitor-binding site of HIF-1α and AKT1 [28, 29]. The binding pose from the compound with a binding affinity lower than −7.0 kcal/mol was selected for residues-ligand interaction using the Biovia Discovery Studio 2019 and molecular dynamics analysis [30, 31].

2.7 Molecular dynamics

Molecular dynamics was analyzed using the YASARA 20.12.24 program [32] under the AMBER14 forcefield [33]. The environment setting for the simulations was as follows: 310 K for temperature, 1 bar for pressure, 0.997 for water density, 0.9% for NaCl concentration, pH 7.4, and cubic simulation box. The structural flexibility and integrity were analyzed using the root-mean-square deviation (RMSD) of the atomic positions and the root-mean-square fluctuations (RMSF) of the residue positions. The free-binding energy was also calculated using molecular mechanics Poisson–Boltzmann surface area equations [34] in YASARA binding energy macros.

3 Results

3.1 *Effect of DGC, DGT, and DGC + DGT Administration on CT-1, STAT3, BNP, and GATA4*

The MetS group consistently displayed a higher expression of all experimental parameters, i.e., *CT-1*, *STAT3*, *BNP*, and *GATA4*, compared with the N group. The administration of DGT or DGC alone significantly decreased the expression of *CT-1*, and the combination of the two extracts rescued the expression to the levels of the N group (Fig. 1A). The same event was observed for *STAT3* expression, where the administration of DGT, DGC, and DGT + DGC rescued the condition by suppressing the expression as well as the normal condition (Fig. 1B). The protective effect of the treatment was also shown by the alleviation of *BNP* expression compared with that in the MetS group ($p < 0.05$). Interestingly, the

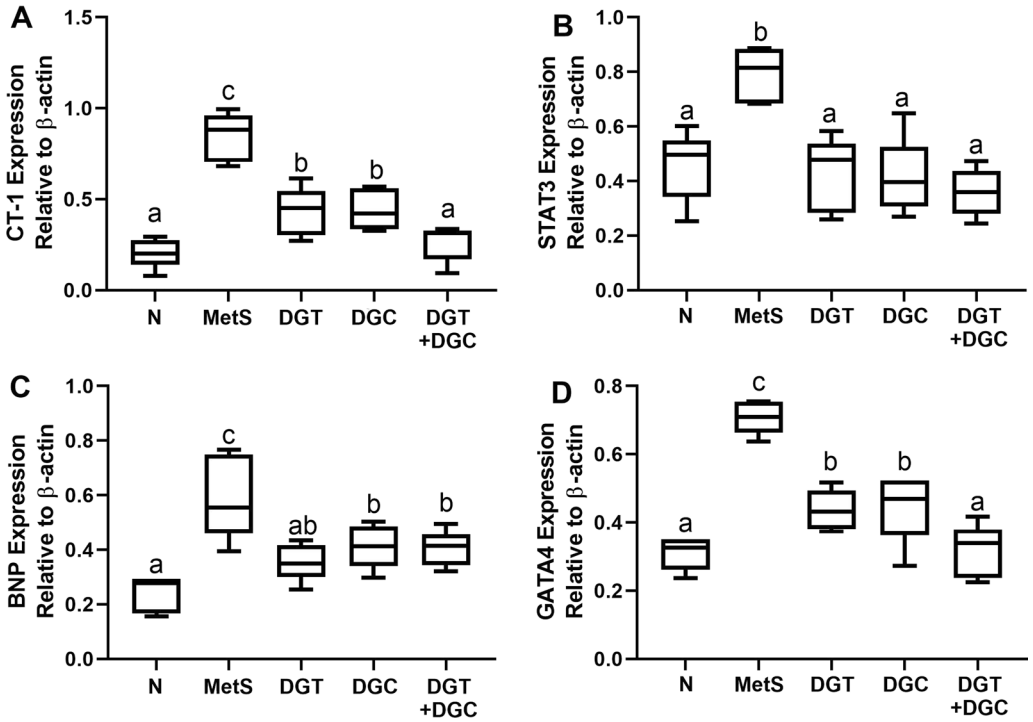

Fig. 1 The expression of *CT-1* (**A**), *STAT3* (**B**), *BNP* (**C**), and *GATA4* (**D**) in each treatment group. Different notation describes a significant difference according to Duncan post-hoc test

administration of DGT alone was statistically similar to that in the N group (Fig. 1C). Furthermore, down-regulation of *GATA4* was also observed in all treated groups, with the DGC + DGT group performing better to overwhelm the expression of *GATA4* as the N group than DGT or DGC alone (Fig. 1D). In summary, the administration of DGT, DGC, or DGT + DGC markedly decreased the expression of the selected parameters below the MetS group.

3.2 Interaction of compounds in DGT and DGC with HIF-1α and AKT1

The compounds from DGT and DGC have a greater affinity for AKT1 than for HIF-1α. Cafestol achieved the lowest binding energy to HIF-1α, whereas ECG posed a minor energy requirement to bind to AKT1. Furthermore, not all analyzed compounds showed a low binding energy with AKT1. Only cafestol, chlorogenic acid, kahweol, EC, ECG, EGC, and EGCG showed small binding energy (lower than − 7.0 kcal/mol) to AKT1. In addition, cafestol, ECG, and EGCG displayed similar binding energies with the Inhibitor-8, a known inhibitor of AKT1 (Table 2). Therefore, the compounds with binding energy smaller than − 7.0 kcal/mol were used for residue binding analysis.

Table 2 The binding energy of compounds from GT and GC from the molecular docking analysis

Compound	Binding energy (kcal/mol)	
	HIF1A	AKT1
Cafestol	− 5.0	− 10.1
Chlorogenic acid	− 4.5	− 9.3
Citric acid	− 3.2	− 5.6
Kahweol	− 4.9	− 9.8
Quinic acid	− 3.5	− 6.2
Trigonelline	− 3.4	− 5.4
EC	− 4.5	− 9.1
ECG	− 3.9	− 10.9
EGC	− 4.3	− 9.0
EGCG	− 4.2	− 10.7
Inhibitor-AKT	–	− 14.1

Compounds with low binding energy exhibited a more significant number of hydrogen and hydrophobic bonds. From the residues-binding point of view, cafestol had the most similar bounded residues with the Inhibitor-8. However, cafestol had fewer hydrogen bonds than chlorogenic acid, EC, ECG, and EGCG. As displayed by the binding energy value, Inhibitor-8 had a more complex

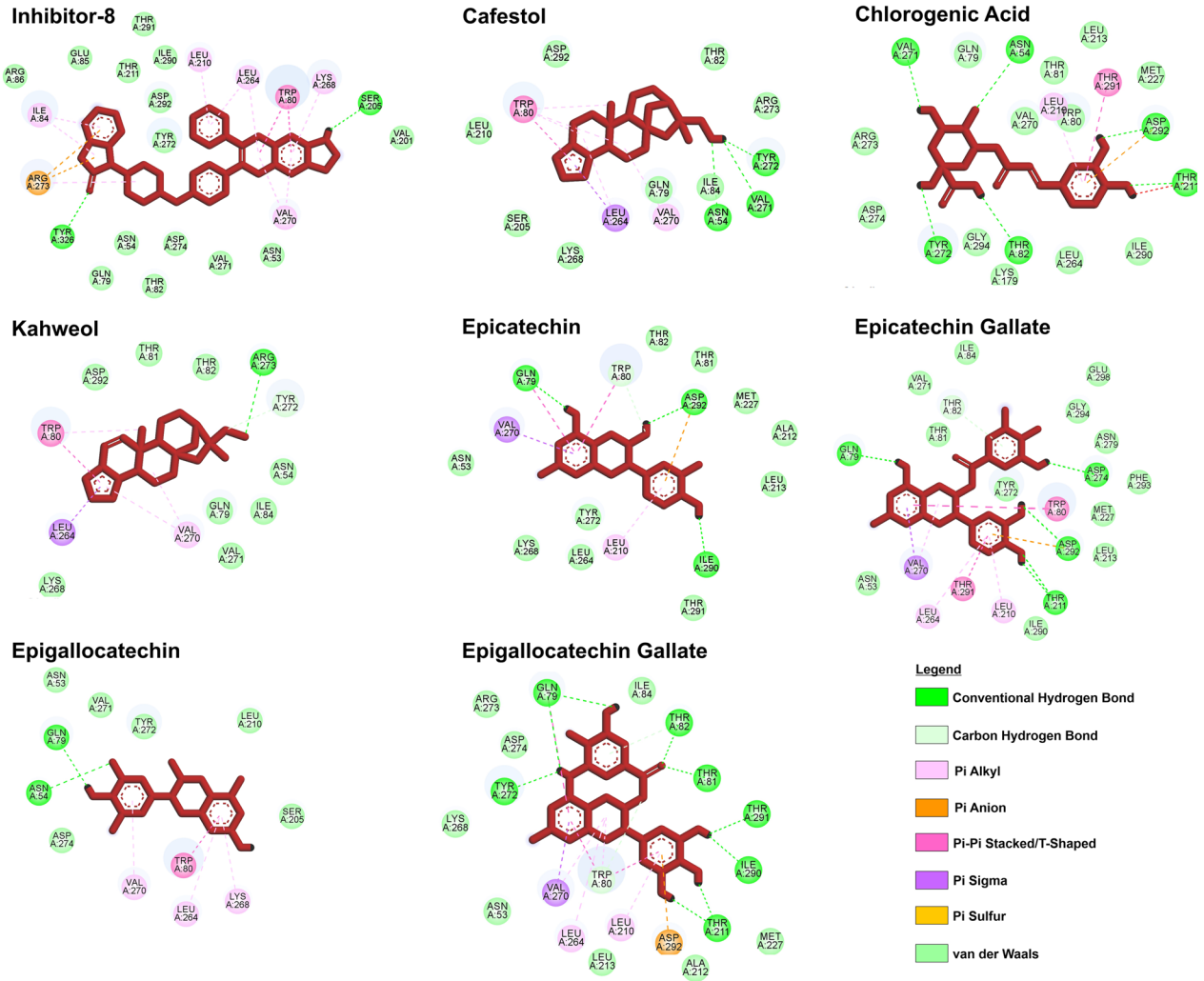

Fig. 2 The residues and interaction chemistry that involved in the protein–ligand binding of selected compounds from GT and GC with AKT1

binding interaction with several hydrogen bonds, hydrophobic bonds, and van der Waals interaction. EC and EGCG was the compound with the more number of hydrogen bonds (Fig. 2). Those compounds were then directed for molecular dynamics simulation to assess the structural and interaction stability in the physiological milieu.

The value of the RMSD atom backbone described that kahweol affected the structural integrity of AKT1, depicted by the high fluctuation of the RMSD value. Other compounds did not affect the structural integrity of AKT1's structure, although several compounds showed some escalation at the end of the simulation, such as chlorogenic acid and EGC (Fig. 3A). The compounds' structure was also stable during the simulation, even though chlorogenic acid displayed the highest RMSD value (Fig. 3B). Furthermore, the RMSD of ligand movement also visualized a stable interaction between the compounds and the AKT1 structure. Kahweol and EC showed similar stability to Inhibitor-8 (Fig. 3C). This observation was also supported by the number of hydrogen bonds in the complexes, which had a similar event without any significant difference (Fig. 3D). However, the RMSF value described the instability of some residues of AKT1, including VAL45, GLN113, ARG200, GLU298, and VAL429. Those instabilities mostly occurred by chlorogenic acid binding to the AKT1 (Fig. 3E). Nevertheless, those instabilities may not affect the interaction of the compounds with the AKT1 according to the free-binding energy calculation. No apparent difference was observed among the simulated complexes, and each complex showed stable binding without any differences in their binding energy (Fig. 3F).

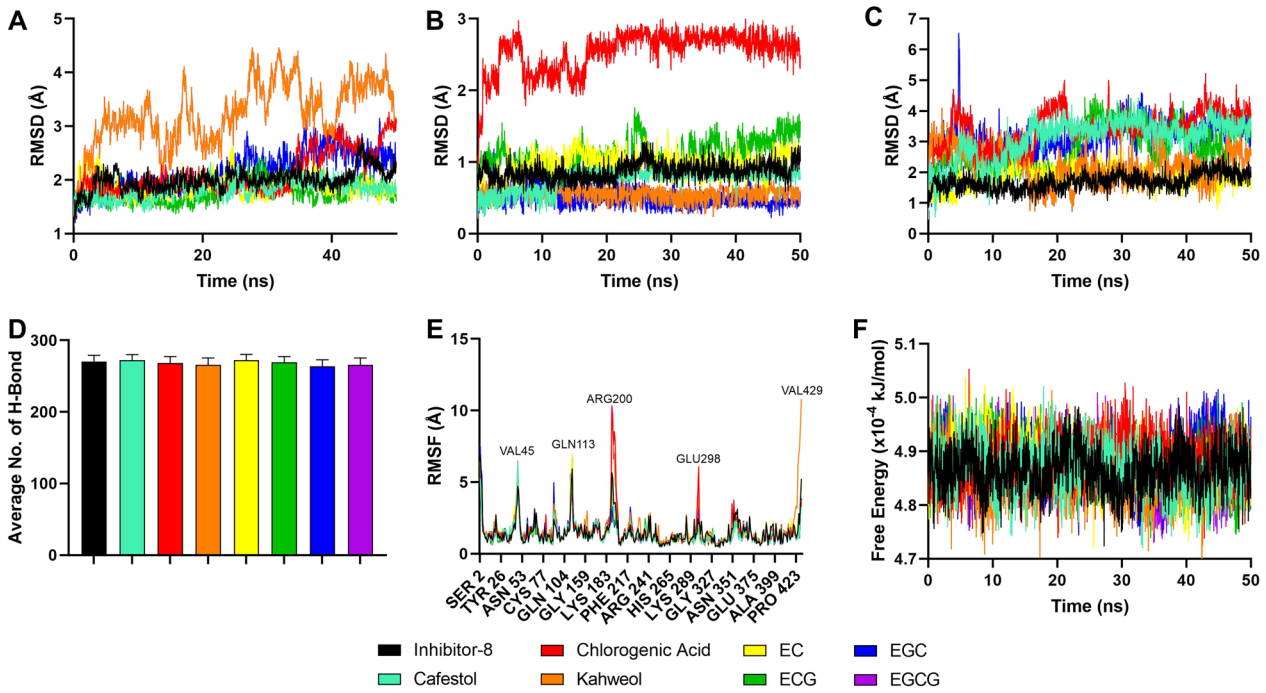

Fig. 3 The structural dynamics of protein, ligand, and the interaction among them. The RMSD of atom backbone (**A**), the RMSD of ligand structure (**B**), the RMSD of ligand movement (**C**), the average number of hydrogen bond (**D**), the RMSF of each residue of AKT1 (**E**), and the free-binding energy of each complex (**F**)

4 Discussion

CVD has become a common medical manifestation of MetS. Several biomarkers have been discovered to detect cardiac dysfunction, and BNP has become an accurate predictor [35]. Increased level of BNP provides a robust prediction of cardiac dysfunction [36, 37]. This study confirmed that event where the MetS group had higher *BNP* levels than the N group. Fortunately, the administration of DGC, DGT, and a combination of the two could restore the expression of *BNP* near the N condition (Fig. 1C). Thus, the DGT + DGC could contribute to cardio-protective effect under MetS conditions.

Since the transcription factor GATA4 regulates *BNP* expression [11], this study also measured its expression. In line with the *BNP* result, MetS increased the expression of *GATA4*, and the administration of DGT, DGC, particularly DGT + DGC, downregulated *GATA4*'s expression (Fig. 1D). Therefore, the GATA4 expression regulator was also measured to comprehend the upstream target of the current treatment. Previously, *GATA4* expression was upregulated by *STAT3* expression. [10] Thus, *STAT3* was also evaluated to confirm the regulatory mechanism of the treatment. During the *GATA4* regulation, *STAT3* is also repressed upon treatment as an N condition (Fig. 1B). *CT-1* expression was also evaluated to better understand the modulatory mechanism of the treatment of the MetS condition, mainly related to CVD. As previously described, CT-1 activates the STAT3 upon binding to gp130. Thus, the upregulation of CT-1 expression may influence *STAT3*'s expression.

Interestingly, the results showed the same manner of lower expression of *CT-1* in the N group than in MetS. The DGC and DGT treatment diminished *CT-1* expression, with DGT + DGC administration performing better in reducing *CT-1* expression in the N group (Fig. 1A). According to the data, the expression of *BNP* in MetS was CT-1-dependent. However, the downregulation of *CT-1* post-treatment still needs further explanation to clearly define the cardio-protective effect DGT, DGC, and DGT + DGC.

A previous study demonstrated that the increasing level of CT-1 induced by hypoxic stress suggests the involvement of HIF-1α in CVD events [38]. This condition was confirmed by a previous study that reported that HIF-1α dependently regulated CT-1 expression at the transcriptional level [39]. Unfortunately, the computational analysis failed to define the cardio-protective activity through the HIF-1α axis. All compounds from DGT and DGC failed to bind with HIF-1α to perform their inhibitory activity (Table 2). Thus, another upstream target may be involved in the modulatory activity of the above-mentioned parameters.

The regulation of hypoxia can be achieved through indirect regulation of HIF-1α. The resistance to hypoxia is also achieved through AKT1 signaling [40]. AKT1 dictates the expression of HIF-1α, and inhibition of AKT1 resulted in the alleviation of HIF-1α expression [41]. Hence, AKT1 may encompass the regulatory mechanism of DGT, DGC, and DGT + DGC treatment. Fortuitously, most of the compounds from GT and GC could interact with AKT1 at its inhibitory site. Cafestol, chlorogenic acid, kahweol, EC, ECG, EGC, and EGCG bound to AKT1 near the Inhibitor-8, a known inhibitor for AKT1 (Table 2, Fig. 2). Molecular dynamics simulations also complement the evidence by showing stable binding of those compounds to perform an inhibitory activity (Fig. 3). Kahweol also affected the structural integrity of AKT1 with great binding affinity, as shown in the RMSD of ligand movement and free-binding energy calculations. Other compounds above also perform excellent binding to the allosteric inhibition site of AKT1 as Inhibitor-8. The inhibition of AKT1 by those compounds may alter the AKT1 ability to induce HIF-1α expression. The low level of HIF-1α directly suppresses the CT-1, STAT3, GATA4, and BNP expression, consecutively. As a result, a low level of BNP will repair cardiac function. Therefore, the DGT, DGC, and DGT + DGC may exhibit their cardio-protective activity through indirect CT-1 expression regulation by inhibiting AKT1 activity. Nevertheless, the measurement of HIF-1α expression was not measured in this study. The measurement of HIF-1α along with the AKT1 expression will further clarify the association of AKT1 inhibition to regulate CT-1 through AKT1 and HIF-1α axis. In addition, the use of quantitative Real-Time Polymerase Chain Reaction (qRT-PCR) also needed to confirm the current results.

5 Conclusions

MetS upregulated *CT-1*, *STAT3*, *GATA4*, and *BNP*, while treatment with DGT, DGC, and DGT + DGC decreased the expression of these genes. The protective role of DGT, DGC, and DGT + DGC may occur through AKT1 inhibition by several bioactive components, mainly cafestol, chlorogenic acid, kahweol, EC, ECG, EGC, and EGCG. The DGT + DGC provided better bioactivity by regulating the expression as the N level.

Abbreviations

CVD	Cardiovascular diseases
MetS	Metabolic syndrome
IR	Insulin resistance
DGT	Decaffeinated green tea
DGC	Decaffeinated green coffee
DGT + DGC	Decaffeinated green tea and decaffeinated green coffee combination
CT-1	Cardiotrophin-1
STAT3	Signal transducer and activator of transcription 3
GATA4	GATA binding protein 4
BNP	B-type natriuretic peptide
HIF-1α	Hypoxia-inducible factor 1-alpha
AKT1	RAC-alpha serine/threonine-protein kinase
IL-6	Interleukin-6
gp130	Membrane glycoprotein 130
HFHS	High-fat and high-sucrose
STZ	Streptozotocin
3D	Three-dimension
EC	Epicatechin
ECG	Epicatechin gallate
EGC	Epigallocatechin
EGCG	Epigallocatechin gallate
PDB	Protein data bank
RMSD	Root-mean-square deviation
RMSF	Root-mean-square fluctuations
qRT-PCR	Quantitative real-time polymerase chain reaction

Acknowledgments

The authors thank the laboratory assistant of the Laboratory of Animal Physiology, Structure, and Development, Department of Biology, Brawijaya University, for their technical assistance during the experiments. The authors also thank to Dwi Adi Nugroho for the advice during the study, Adrian Pearl Gunawan, Evalina Izzatur Rochmah, Adinda Nabila Azzah, Andi Nurul Isri Indriany Idhil, Fuad Abdullah for reviewing of the Journal article.

Author contributions

MSR and ML conceived and designed the study. MNK, NAW, BRC, and FEH performed the experiments. BRC, FEH, and NW wrote, reviewed, and edited the manuscript. All authors read and approved the final manuscript.

Funding

This project was financially supported by the Ministry of Education, Culture, Research, and Technology, Republic of Indonesia (Grant No. 1071.37/UN10.C10/TU/2022).

Availability of data and material

Not applicable.

Declarations

Ethics approval and consent to participate

This study was approved ethically by the Ethical Committee of the Faculty of Medicine, Brawijaya University, Malang, East Java, Indonesia (Reference no. 148 /EC /KEPK–S2 /06 /2021).

Consent for publication

Not applicable.

Competing interests

None.

Author details

[1]Department of Cardiology and Vascular Medicine, Faculty of Medicine, Brawijaya University, Malang, East Java 65145, Indonesia. [2]Cardiovascular Research Center, Brawijaya University, Malang, East Java 65145, Indonesia. [3]School of Nursing, Faculty of Health Sciences, Brawijaya University, Malang, East Java 65145, Indonesia. [4]Master Program of Biomedical Sciences, Faculty of Medicine, Brawijaya University, Malang, East Java 65145, Indonesia. [5]Faculty of Animal Sciences, Brawijaya University, Malang, East Java 65145, Indonesia. [6]Bioinformatics Research Center, Indonesian Institute of Bioinformatics (INBIO Indonesia), Malang, East Java 65145, Indonesia. [7]School of Population Health, Faculty of Medicine, University of New South Wales, Samuels Building, F25, Samuel Terry Ave, Kensington, NSW, 2033, Sydney, Australia. [8]Department of Biology, Faculty of Mathematics and Natural Sciences, Brawijaya University, East Java 65145 Malang, Indonesia.

Received: 1 December 2022 Accepted: 1 May 2023
Published online: 26 May 2023

References

1. Saklayen MG (2018) The global epidemic of the metabolic syndrome. Curr Hypertens Rep 20:12. https://doi.org/10.1007/s11906-018-0812-z
2. Suliga E, Ciesla E, Lelonek M et al (2022) Lifestyle elements and risk of metabolic syndrome in adults. PLoS ONE 17:e0275510. https://doi.org/10.1371/journal.pone.0275510
3. Tune JD, Goodwill AG, Sassoon DJ, Mather KJ (2017) Cardiovascular consequences of metabolic syndrome. Transl Res 183:57–70. https://doi.org/10.1016/j.trsl.2017.01.001
4. Moreno-Aliaga MJ, Romero-Lozano MA, Castaño D et al (2012) Role of cardiotrophin-1 in obesity and insulin resistance. Adipocyte 1:112–115. https://doi.org/10.4161/adip.19696
5. Watanabe T, Konii H, Sato K (2018) Emerging roles of cardiotrophin-1 in the pathogenesis and biomarker of atherosclerosis. J 1:94–105. https://doi.org/10.3390/j1010010
6. Asrih M, Mach F, Quercioli A et al (2013) Update on the pathophysiological activities of the cardiac molecule cardiotrophin-1 in obesity. Mediators Inflamm 2013:370715. https://doi.org/10.1155/2013/370715
7. Sharif S, Saleem A, Naz S et al (2021) Increased expression of cardiotrophin-1 in cardiomyopathy patients. Balkan J Med Genet 24:21–26. https://doi.org/10.2478/bjmg-2021-0008
8. Chandrasekar B, Melby PC, Pennica D, Freeman GL (1998) Overexpression of cardiotrophin-1 and gp130 during experimental acute Chagasic cardiomyopathy. Immunol Lett 61:89–95. https://doi.org/10.1016/s0165-2478(97)00167-3
9. Qi Q-R, Yang Z-M (2014) Regulation and function of signal transducer and activator of transcription 3. World J Biol Chem 5:231–239. https://doi.org/10.4331/wjbc.v5.i2.231
10. Snyder M, Huang X-Y, Zhang JJ (2010) Stat3 directly controls the expression of Tbx5, Nkx2.5, and GATA4 and is essential for cardiomyocyte differentiation of P19CL6 cells. J Biol Chem 285:23639–23646. https://doi.org/10.1074/jbc.M110.101063
11. McBride K, Nemer M (2001) Regulation of the ANF and BNP promoters by GATA factors: lessons learned for cardiac transcription. Can J Physiol Pharmacol 79:673–681
12. Stewart RAH, Kirby A, White HD et al (2022) B-type natriuretic peptide and long-term cardiovascular mortality in patients with coronary heart disease. J Am Heart Assoc 11:e024616. https://doi.org/10.1161/JAHA.121.024616
13. Castro-Barquero S, Ruiz-León AM, Sierra-Pérez M et al (2020) Dietary strategies for metabolic syndrome: a comprehensive review. Nutrients 12:2983. https://doi.org/10.3390/nu12102983
14. Esmaeelpanah E, Razavi BM, Hosseinzadeh H (2021) Green tea and metabolic syndrome: a 10-year research update review. Iran J Basic Med Sci 24:1159–1172. https://doi.org/10.22038/IJBMS.2021.52980.11943
15. Bhandarkar NS, Mouatt P, Brown L, Panchal SK (2019) Green coffee ameliorates components of diet-induced metabolic syndrome in rats. J Funct Foods 57:141–149. https://doi.org/10.1016/j.jff.2019.04.003
16. Roshan H, Nikpayam O, Sedaghat M, Sohrab G (2018) Effects of green coffee extract supplementation on anthropometric indices, glycaemic control, blood pressure, lipid profile, insulin resistance and appetite in patients with the metabolic syndrome: a randomised clinical trial. Br J Nutr 119:250–258. https://doi.org/10.1017/S0007114517003439
17. Rohman MS, Lukitasari M, Nugroho DA et al (2021) Decaffeinated light-roasted green coffee and green tea extract combination improved metabolic parameters and modulated inflammatory genes in metabolic syndrome rats. F1000 Res 10:467
18. Lukitasari M, Nugroho DA, Rohman MS et al (2020) Beneficial effects of green coffee and green tea extract combination on metabolic syndrome improvement by affecting AMPK and PPAR-α gene expression. J Adv Pharm Technol Res 11:81–85. https://doi.org/10.4103/japtr.JAPTR_116_19
19. Lukitasari M, Rohman MS, Nugroho DA et al (2021) Green tea and decaffeinated light roasted green coffee extract combination improved cardiac insulin resistance through free fatty acids and adiponectin/FAS pathway amelioration in metabolic syndrome rat model. F1000 Res 10:990
20. Rachmawati E, Rohman MS, Sargowo D et al (2021) Decaffeinated coffee and green tea extract inhibit foam cell atherosclerosis by lowering inflammation and improving cholesterol influx/efflux balance through upregulation of PPARγ and miR-155. F1000 Res 10:1175
21. Rohman MS, Sishartami LW, Widodo N et al (2022) The combination of decaffeinated coffee (*Coffea canephora*) and Green Tea (*Camellia sinensis*) reduced PSGL-1 glycosylation by GALNT2 in Ox-LDL-induced RAW 264.7. Int J Nutr Pharmacol Neurol Dis 12:112. https://doi.org/10.4103/ijnpnd.ijnpnd_7_22
22. Rohman MS, Lukitasari M, Nugroho DA et al (2017) Development of an experimental model of metabolic syndrome in Sprague Dawley rat. Res J Life Sci 4:76–86
23. Wei F, Tanokura M (2015) Chapter 17—organic compounds in green coffee beans. In: Preedy VR (ed) Coffee in health and disease prevention. Academic Press, San Diego, pp 149–162
24. Rachmawati E, Rohman S, Sishartami L et al (2022) In silico modelling, regulation of cell viability and anti atherosclerotic effect in macrophage by decaffeinated coffee and green tea extract. Pharmacogn J 14:46–55. https://doi.org/10.5530/pj.2022.14.7
25. Trott O, Olson AJ (2010) AutoDock Vina: improving the speed and accuracy of docking with a new scoring function, efficient optimization and multithreading. J Comput Chem 31:455–461. https://doi.org/10.1002/jcc.21334
26. Dallakyan S, Olson AJ (2015) Small-molecule library screening by docking with PyRx. Methods Mol Biol 1263:243–250. https://doi.org/10.1007/978-1-4939-2269-7_19
27. O'Boyle NM, Banck M, James CA et al (2011) Open Babel: an open chemical toolbox. J Cheminform 3:33. https://doi.org/10.1186/1758-2946-3-33
28. Cardoso R, Love R, Nilsson CL et al (2012) Identification of Cys255 in HIF-1α as a novel site for development of covalent inhibitors of HIF-1α/ARNT PasB domain protein-protein interaction. Protein Sci 21:1885–1896. https://doi.org/10.1002/pro.2172
29. Wu W-I, Voegtli WC, Sturgis HL et al (2010) Crystal structure of human AKT1 with an allosteric inhibitor reveals a new mode of kinase inhibition. PLoS ONE 5:e12913. https://doi.org/10.1371/journal.pone.0012913
30. Hermanto FE, Warsito W, Rifa'i M, Widodo N (2022) On the hypolipidemic activity of elicited soybeans: evidences based on computational analysis. Indones J Chem 22:1626–1636. https://doi.org/10.22146/ijc.75777
31. Nguyen NT, Nguyen TH, Pham TNH et al (2020) Autodock vina adopts more accurate binding poses but autodock4 forms better binding affinity. J Chem Inf Model 60:204–211. https://doi.org/10.1021/acs.jcim.9b00778
32. Krieger E, Vriend G (2015) New ways to boost molecular dynamics simulations. J Comput Chem 36:996–1007. https://doi.org/10.1002/jcc.23899
33. Maier JA, Martinez C, Kasavajhala K et al (2015) ff14SB: improving the accuracy of protein side chain and backbone parameters from ff99SB. J Chem Theory Comput 11:3696–3713. https://doi.org/10.1021/acs.jctc.5b00255
34. Miller BR, McGee TD, Swails JM et al (2012) MMPBSA.py: an efficient program for end-state free energy calculations. J Chem Theory Comput 8:3314–3321. https://doi.org/10.1021/ct300418h
35. Burke MA, Cotts WG (2007) Interpretation of B-type natriuretic peptide in cardiac disease and other comorbid conditions. Heart Fail Rev 12:23–36. https://doi.org/10.1007/s10741-007-9002-9
36. Santhekadur PK, Kumar DP, Seneshaw M et al (2017) The multifaceted role of natriuretic peptides in metabolic syndrome. Biomed Pharmacother 92:826–835. https://doi.org/10.1016/j.biopha.2017.05.136
37. Christoffersen C, Goetze JP, Bartels ED et al (2002) Chamber-dependent expression of brain natriuretic peptide and its mRNA in normal and diabetic pig heart. Hypertension 40:54–60. https://doi.org/10.1161/01.HYP.0000021780.21830.DD
38. Hishinuma S, Funamoto M, Fujio Y et al (1999) Hypoxic stress induces cardiotrophin-1 expression in cardiac myocytes. Biochem Biophys Res Commun 264:436–440. https://doi.org/10.1006/bbrc.1999.1535
39. Robador PA, San José G, Rodríguez C et al (2011) HIF-1-mediated up-regulation of cardiotrophin-1 is involved in the survival response of cardiomyocytes to hypoxia. Cardiovasc Res 92:247–255. https://doi.org/10.1093/cvr/cvr202
40. Zhang Z, Yao L, Yang J et al (2018) PI3K/Akt and HIF-1 signaling pathway in hypoxia-ischemia. Mol Med Rep 18:3547–3554. https://doi.org/10.3892/mmr.2018.9375
41. Fu B, Xue J, Li Z et al (2007) Chrysin inhibits expression of hypoxia-inducible factor-1alpha through reducing hypoxia-inducible factor-1alpha stability and inhibiting its protein synthesis. Mol Cancer Ther 6:220–226. https://doi.org/10.1158/1535-7163.MCT-06-0526

Publisher's Note